

Oyston *et al* 2021

1 **Title:** Rapid and automated quantification of TDP-43 and FUS mislocalisation for screening
2 of frontotemporal dementia and amyotrophic lateral sclerosis gene variants

3

4 Lisa J. Oyston¹, Stephanie Ubiparipovic^{1,2}, Lauren Fitzpatrick¹, Marianne Hallupp¹, Lauren
5 M. Boccanfuso¹, John B. Kwok¹, Carol Dobson-Stone^{1*}

6

7 ¹The University of Sydney, Brain and Mind Centre and School of Medical Sciences, Faculty
8 of Medicine and Health, Camperdown, NSW 2006, Australia

9 ²Garvan Institute of Medical Research, Darlinghurst, NSW 2010, Australia

10

11 ***Corresponding author: Carol Dobson-Stone**

12 Email: carol.dobson-stone@sydney.edu.au

13 Phone: +61 2 9351 0822

14 Address: Brain and Mind Centre, University of Sydney, 94 Mallett St, Camperdown NSW
15 2050, Australia

16

17

18 *Oyston et al 2021*

19 **Abstract**

20 **Background:** Identified genetic mutations cause 20% of frontotemporal dementia (FTD) and
21 5-10% of amyotrophic lateral sclerosis (ALS) cases: however, for the remainder of patients
22 the origin of the disease is uncertain. The overlap in genetic, clinical and pathological
23 presentation of FTD and ALS suggests these two diseases are related. Post-mortem, 97% of
24 ALS and ~50% of FTD patients show redistribution of the nuclear proteins TDP-43 or FUS
25 to the cytoplasm within affected neurons. We exploited this predominant neuropathological
26 feature to develop an automated method for the quantification of cytoplasmic TDP-43 and
27 FUS in human cell lines.

28 **Results:** Utilising fluorescently-tagged cDNA constructs to identify cells of interest, the
29 fluorescence intensity of TDP-43 or FUS was measured in the nucleus and cytoplasm of
30 HEK293 and SH-SY5Y cells. Confocal microscope images were input into the freely
31 available software CellProfiler, which was used to isolate and measure the two cellular
32 compartments. Significant increases in the amount of cytoplasmic TDP-43 and FUS were
33 detectable in cells expressing known ALS-causative *TARDBP* and *FUS* gene mutations.
34 Pharmacological intervention with the apoptosis inducer staurosporine also induced
35 measurable cytoplasmic mislocalisation of endogenous FUS. Additionally, this technique was
36 able to detect the subtler effect of mutation in a secondary gene (*CYLD*) on endogenous TDP-
37 43 localisation.

38 **Conclusions:** These findings validate this methodology as a novel *in vitro* technique for the
39 quantification of TDP-43 or FUS mislocalisation that can be used to assess the pathogenicity
40 of predicted FTD- or ALS-causative mutations.

41 **Keywords:** frontotemporal dementia, amyotrophic lateral sclerosis, motor neurone disease,
42 TDP-43, FUS, mislocalisation, confocal microscopy, CellProfiler

43

Oyston *et al* 2021

44

45 **Background**

46 Frontotemporal dementia (FTD) is one of the most common forms of presenile dementia and
47 involves the progressive degeneration of the frontal and temporal lobes of the brain.
48 Amyotrophic lateral sclerosis (ALS) is a progressive neurodegenerative disorder that affects
49 the upper and lower motor neurons leading to muscle weakness and paralysis [1]. Increasing
50 genetic evidence, neuropathological and clinical observations have identified a substantial
51 overlap between these two disorders [2]. Several genes have been identified where mutations
52 can cause either FTD or ALS (FTD-ALS genes) including *C9orf72*, *VCP*, *OPTN*, *SQSTM1*,
53 *TBK1* [3] and, most recently, *CYLD* [4]. In addition, FTD and ALS share neuropathological
54 similarities: ~95% of ALS and ~50% of FTD patients show cytoplasmic inclusions of the
55 proteins TAR DNA-binding protein 43 (TDP-43) [5, 6] or fused in sarcoma (FUS) within the
56 brain (~5% of ALS and ~10% of FTD patients) [6–8]. In healthy cells, TDP-43 and FUS are
57 largely expressed within the nucleus. In FTD and ALS, affected neurons predominantly
58 display a redistribution of TDP-43 or FUS to the cytoplasm, as well as insoluble TDP-
59 43/FUS aggregates [6, 9, 10]. The importance of TDP-43 and FUS is further demonstrated by
60 the fact that mutation of their encoding genes *TARDBP* and *FUS* is sufficient to cause ALS
61 [7, 11, 12] or, rarely, FTD [13].

62

63 Identified genetic mutations cause 20% of familial FTD and 5-10% of familial ALS cases
64 [14, 15]; however, for the remainder of patients the origin of the disease is uncertain. Despite
65 TDP-43 and/or FUS mislocalisation being a prominent feature in the majority of FTD and
66 ALS cases, including all those carrying FTD-ALS gene mutations [13], this fact has not been
67 applied to the screening of FTD and ALS candidate gene variants on a large scale. In
68 previous studies, TDP-43 and FUS mislocalisation has largely been assessed by subcellular

Oyston *et al* 2021

69 fractionation, immunohistochemistry and manual analysis of confocal microscopy [7, 16–24].
70 Whilst studies utilising these techniques have been informative, these assays are labour
71 intensive, low-throughput, expensive and often produce qualitative data. In addition,
72 microscopy-based techniques could be subject to bias due to manual selection of the cells to
73 be analysed.

74

75 Here we report the development of a rapid and automated technique for the *in vitro* study of
76 TDP-43 and FUS cytoplasmic mislocalisation. TDP-43 or FUS staining in nuclear and
77 cytoplasmic subcellular compartments was measured in thousands of cells from confocal
78 microscope images, using the freely available analysis software CellProfiler [25]. We
79 validated this technique using known genetic and pharmacological drivers of TDP-43 or FUS
80 mislocalisation. We were able to detect increased cytoplasmic localisation of exogenously
81 expressed *FUS* and *TARDBP* mutations relative to wild-type (WT) sequence. We also
82 observed mislocalisation of endogenous FUS upon treatment with the apoptosis inducer
83 staurosporine. Importantly, we could also detect more subtle changes in the cellular
84 distribution of endogenous TDP-43, arising from mutation in a secondary gene (*CYLD*
85 p.M719V). This validated methodology can now be utilised for rapidly assessing the
86 pathogenicity of newly discovered FTD and ALS gene variants by quantifying their effect on
87 TDP-43 and/or FUS localisation.

88

89 **Results**

90 *Detection of FUS cytoplasmic mislocalisation with exogenous expression of FUS mutations*
91 In order to validate our method for the unbiased quantification of FUS and TDP-43
92 mislocalisation we initially utilised known pathogenic *FUS* mutations that drastically alter

Oyston *et al* 2021

93 FUS subcellular localisation [7, 26]. Expression of green fluorescent protein (GFP)-tagged
94 FUS protein with missense mutation R521C (FUS_{R521C}) or truncation mutant FUS_{R495X} in the
95 neuronal-like neuroblastoma cell line, SH-SY5Y, led to a significant increase in the
96 fluorescence intensity of cytoplasmic FUS (**Fig. 1e-k**) when compared to FUS_{WT} (**Fig. 1a-c**,
97 **h**). This increase in cytoplasmic FUS was accompanied by a corresponding decrease in the
98 fluorescence intensity of nuclear FUS (**Fig. 1d**). Together, these resulted in a 9.5- and 12.5-
99 fold increase in the FUS cytoplasmic/nuclear ratio for cells expressing FUS_{R521C} (0.97 ± 0.04 ;
100 $p < 0.0001$) and FUS_{R495X} (1.28 ± 0.04 ; $p < 0.0001$), respectively, relative to FUS_{WT} (0.10 ± 0.00 ;
101 **Fig. 1l**). Similar results were found when overexpressing the FUS_{R521C} (1.04 ± 0.05 ; $p < 0.0001$)
102 and FUS_{R495X} (1.81 ± 0.10 ; $p < 0.0001$) mutants in human embryonic kidney (HEK293) cells
103 (**Fig. S1**), although the decrease in nuclear fluorescence intensity of FUS was not as
104 prominent (**Fig. S1d**).

105

106 *Detection of endogenous FUS cytoplasmic mislocalisation following staurosporine treatment*
107 To test our ability to quantify the subcellular distribution of endogenous FUS we utilised the
108 apoptosis inducer staurosporine, which has been previously reported to cause cytoplasmic
109 mislocalisation of FUS [16]. Application of increasing doses of staurosporine showed an
110 increase in the fluorescence intensity of cytoplasmic FUS in cells treated with the two highest
111 dose of staurosporine (1 and 10 μ M; **Fig. 2c-d, f**). A corresponding decrease in the nuclear
112 intensity of FUS was also seen in SH-SY5Y cells (**Fig. 2e**). There was a significant increase
113 of cytoplasmic/nuclear FUS ratio for all treatment groups (0.1μ M: 0.13 ± 0.01 ; $p = 0.0405$; 1
114 μ M: 0.31 ± 0.06 ; $p = 0.0152$; 10μ M: 1.35 ± 0.07 ; $p = 0.0002$) relative to untreated cells
115 (0.09 ± 0.00 ; **Fig. 2g**). HEK293 cells treated with staurosporine also exhibited a dose-response
116 effect on FUS subcellular localisation. In general, HEK293 cells were more tolerant of the

Oyston *et al* 2021

117 staurosporine treatment (**Fig. S2a-d**) as shown by the lower cytoplasmic/nuclear ratios
118 observed when compared to the SH-SY5Y cells (**Fig. 2g** and **S2g**). Treatment with 10 M
119 staurosporine caused the majority of FUS to be present in the cytoplasm rather than the
120 nucleus in SH-SY5Y cells (1.35 ± 0.07 ; $p=0.0002$; **Fig. 2d, g**) whilst the same treatment in the
121 HEK293 cells caused only a small proportion of FUS protein to be mislocalised (0.28 ± 0.01 ;
122 $p<0.0001$; **Fig. S2d, g**). Despite these differences in effect size, we could detect a significant
123 effect of staurosporine treatment on mislocalisation of endogenous FUS in both cell lines.

124

125 *Detection of TDP-43 cytoplasmic mislocalisation with exogenous expression of TARDBP*
126 *mutations*

127 We took the same initial approach used for FUS to validate this method for the quantification
128 of TDP-43 cytoplasmic mislocalisation: i.e. exogenous expression of known pathogenic
129 mutations in *TARDBP*. We examined p.A315T, one of the earliest detected and thus most
130 extensively examined mutations [27–29], and two of the mutations most commonly observed
131 in ALS patients: p.M337V and p.A382T [11, 28–30].

132

133 In SH-SY5Y cells, a significant increase in the cytoplasmic/nuclear ratio of GFP-tagged
134 TDP-43_{A315T} (0.87 ± 0.01 ; $p=0.0016$; **Fig. 3b, f, k**) and TDP-43_{A382T} (0.86 ± 0.02 ; $p=0.0032$;
135 **Fig. 3d, h, k**) was observed when compared to TDP-43_{WT} (0.75 ± 0.01 ; **Fig. 3a, e, k**). In
136 contrast, there was a significant decrease in the cytoplasmic/nuclear ratio of GFP-tagged
137 TDP-43_{M337V} (0.63 ± 0.01 ; $p=0.0028$; **Fig. 3c, g, k**) relative to TDP-43_{WT}. Similar to the
138 experiments with FUS, expression of TDP-43 mutations had a lesser effect in HEK293 cells
139 (**Fig. S3**). Once again, there was a significant increase in the cytoplasmic/nuclear ratio of

Oyston *et al* 2021

140 TDP-43_{A315T} (0.57±0.02; p=0.0021; **Fig. S3b, f, k**) and TDP-43_{A382T} cells (0.66±0.03;
141 p=0.0026; **Fig. S3d, h, k**) when compared to TDP-43_{WT} (0.50±0.02; **Fig. S3a, e, k**).
142 However, no significant effect was observed in TDP-43_{M337V} cells (0.52±0.01; **Fig. S3c, g,**
143 **k**).

144

145 *Detection of endogenous TDP-43 cytoplasmic mislocalisation in cells expressing a causative*
146 *FTD/ALS mutation*

147 To demonstrate the potential of this methodology for evaluating the pathogenicity of variants
148 in other FTD/ALS genes, we expressed a known familial FTD/ALS-causative mutation in the
149 CYLD gene, p.M719V [4], and observed the changes in endogenous TDP-43 localisation.
150 We previously determined that overexpression of CYLD_{M719V} increases the proportion of
151 cytoplasmic TDP-43-positive mouse primary cortical neurons by ~20% when compared to
152 CYLD_{WT} [4]. When compared to GFP-only vector control (0.079±0.001; **Fig. 4a-d**),
153 expression of CYLD_{WT}-GFP (**Fig. 4e-h**) in SH-SY5Y cells led to a significant 1.2-fold
154 increase in the TDP-43 cytoplasmic/nuclear ratio (0.095±0.001; p=0.0002; **Fig. 4s**). In turn,
155 expression of CYLD_{M719V}-GFP (**Fig. 4m-p**) caused a further 1.3-fold increase in
156 cytoplasmic/nuclear TDP-43 relative to CYLD_{WT}-GFP (0.121±0.002; p<0.0001). The
157 CYLD_{M719V} mutation had the same effect in HEK293 cells, causing a 1.3-fold increase in the
158 cytoplasmic/nuclear ratio relative to CYLD_{WT} (0.145±0.007; p=0.0115; **Fig. S4e-h, m-p, s**).
159 We also transfected cells with the CYLD_{D681G} mutation (**Fig. 4i-l**, **Fig. S4i-l**) which is
160 catalytically inactive and known to cause CYLD cutaneous syndrome, a skin tumour disorder
161 [31, 32]. Our data corroborated previous results [4] that the CYLD_{D681G} mutation had no
162 effect on TDP-43 localisation when compared to the GFP-only vector control in either cell
163 type (**Fig. 4s**, **Fig S4s**).

Oyston *et al* 2021

164

165 **Discussion**

166 In this study we have validated a novel methodology for the automated quantification of
167 cytoplasmic TDP-43 and FUS in human cell lines under three different experimental
168 paradigms: determining localisation of exogenously expressed mutant TDP-43 or FUS;
169 detecting the effect of a chemical modulator on endogenous FUS localisation; and detecting
170 the effect of a secondary gene on endogenous TDP-43 localisation. This rapid, cheap,
171 quantitative assay can now be utilised for rapidly assessing drug treatments and the
172 pathogenicity of newly discovered FTD and ALS gene variants by quantifying their effect on
173 TDP-43 and/or FUS localisation.

174

175 Previous studies examining TDP-43 and FUS have quantified cytoplasmic mislocalisation in
176 different ways. Many studies have reported the proportion of the cell population that display
177 cytoplasmic TDP-43 or FUS expression [12, 18, 19, 21, 24]. This may present a problem with
178 reproducibility, since fluorescence detection thresholds for considering a cell as 'positive' for
179 cytoplasmic protein likely differ between labs and will vary according to the microscopy
180 equipment used. We selected the ratio of cytoplasmic to nuclear expression as our primary
181 measure, having observed reduced variability between experimental replicates in comparison
182 to individual nuclear and cytoplasmic measurements. Some studies have reported similar
183 measurements using techniques such as high-content screening confocal microscopy to study
184 TDP-43 or FUS mislocalisation under different conditions [33, 34]. Whilst high-content
185 screening allows for a more high-throughput study design than our methodology, the
186 extensive infrastructure required is expensive and can require substantial optimisation.

187

Oyston *et al* 2021

188 Another general observation in our experiments was that SH-SY5Y cells often displayed a
189 greater degree of cytoplasmic mislocalisation than that in HEK293 cells under the same
190 conditions. This may be due to SH-SY5Y cells being a neuronal cell line and thus more
191 disease relevant, or due to the longer transfection time required to achieve optimal
192 transfection efficiency in SH-SY5Y cells (48 hours, versus 24 hours in HEK293), causing
193 additional stress on the cells. It should also be noted that transfection efficiency also dictated
194 the number of images required to reach the desired cell number per replicate (300 cells). SH-
195 SY5Y cells, which had a lower transfection efficiency require more images to achieve the
196 same number of cells for quantification.

197

198 The cytoplasmic mislocalisation and/or aggregation of FUS in neurons and glia of post-
199 mortem tissue from patients with FTD and ALS caused by FUS mutations has been widely
200 established [7, 12, 35, 36]. This pathology has been recapitulated by expression of FUS
201 mutations in mammalian cells [7, 12, 26]. In this study, exogenous expression of the severe
202 truncation mutation FUS_{R495X} caused the majority of FUS to be mislocalised to the cytoplasm
203 as previously demonstrated by Bosco *et al.* [26] using live-cell confocal microscopy and 3D
204 images (11-28 cells). Our quick and simple methodology was able to duplicate these results
205 using 2D images and a larger number of cells (1800 cells total). While we recognise the
206 merits of quantifying the entire cell volume, measuring such a small number of selected cells
207 is not representative of the population and may not be able to detect more subtle or variable
208 effects in protein localisation.

209

210 Expression of the FUS_{R521C} missense mutation and treatment with staurosporine (1-10 μ M)
211 also reproduced previous qualitative microscopy and subcellular fractionation results [7, 16,

Oyston *et al* 2021

212 37] showing a significant increase in the FUS cytoplasmic/nuclear ratio. Confirmation of
213 these results demonstrate the effectiveness of this new methodology in providing quantitative
214 data where previously qualitative or labour-intensive experiments were required. Our ability
215 to quantify FUS cytoplasmic mislocalisation following staurosporine treatment also
216 demonstrates the possibility of this technique for use in testing the ability of novel FTD and
217 ALS drug treatments to modulate FUS or TDP-43 mislocalisation.

218

219 The majority (~95%) of ALS and ~50% of FTD cases are characterised by the abnormal
220 accumulation of TDP-43 in the cytoplasm of neurons and glia, even though in most cases
221 mutations in *TARDBP* are absent [6]. Mutations in TDP-43 have been associated with both
222 FTD and ALS and lead to TDP-43 cytoplasmic mislocalisation [11, 13]. Unlike FUS, the
223 expression of TDP-43 mutations in primary cells and cell lines does not reproduce the
224 dramatic cytoplasmic mislocalisation seen in post-mortem tissue [38–41]. In addition,
225 overexpression of exogenous TDP-43 is sufficient to induce mislocalisation even for WT
226 sequence [19, 23] Any differences between WT and mutant TDP-43 for this characteristic are
227 therefore harder to discern in exogenous expression experiments and may be responsible for
228 differing results being reported for the same mutations. Our technique was able to detect a
229 significant increase in the TDP-43 cytoplasmic/nuclear ratio in TDP-43_{A315T} and TDP-43_{A382T}
230 cells when compared to TDP-43_{WT}. This confirms previous results for TDP-43_{A315T} [18, 19]
231 and TDP-43_{A382T} [42, 43]. The TDP-43_{M337V} variant, which displayed a significant decrease in
232 cytoplasmic TDP-43 in SH-SY5Y cells, has previously been shown to increase cytoplasmic
233 TDP-43 in some [19, 21, 24], but not all studies [22]. We note that TDP-43_{M337V} has been
234 shown to aggregate into nuclear puncta [21], which we observed in our experiments. As these
235 puncta fluoresce at a higher intensity than diffuse TDP-43 expression, this may lead to an
236 overall decrease in cytoplasmic/nuclear fluorescence ratio relative to TDP-43_{WT}. Thus, in

Oyston *et al* 2021

237 some cases quantification of nuclear and cytoplasmic puncta will be a useful adjunct to assess
238 the pathogenicity of a given mutation. We also note that mislocalisation of TDP-43 is not the
239 only mechanism by which *TARDBP* mutations lead to disease: for example, changes in
240 protein stability or interaction partners have also been described [28]. However, we envisage
241 that the mislocalisation assay as implemented here would be a useful tool in a battery of
242 assays to screen novel *TARDBP* variants.

243

244 Lastly, we were able to recapitulate the effect of WT CYLD, the FTD-ALS-causative
245 mutation p.M719V and the catalytically inactive mutation p.D681G on subcellular
246 localisation of endogenous TDP-43, which we previously observed in mouse cortical neurons
247 [4]. In comparison to the other experiments used to validate this quantification method, the
248 degree of change in the endogenous TDP-43 cytoplasmic/nuclear ratio between the empty
249 vector, the CYLD_{WT} and the CYLD mutations was very small: e.g., absolute increase in ratio
250 of ~0.03-0.04 between CYLD_{WT} & CYLD_{M719V} (Fig. 4s. and S4s). Our ability to detect
251 significant differences for such a subtle change demonstrates the sensitivity of this technique
252 for detecting changes in TDP-43 and FUS localisation *in vitro*. The utilisation of our
253 quantification method in this format demonstrates what we believe to be its primary use,
254 validating the pathogenicity of newly identified FTD- or ALS-associated variants in genes
255 other than *FUS* and *TARDBP*.

256

257 **Conclusions**

258 In summary, this study demonstrates a simple automated methodology for quantifying TDP-
259 43 and FUS cytoplasmic mislocalisation *in vitro*. This technique can easily be added to
260 studies utilising qualitative data to strengthen clearly noticeable phenotypes in an unbiased

Oyston *et al* 2021

261 manner, as well as to highlight subtle changes that may have not been previously identified.
262 Utilisation of this technique to aid in assessing pathogenicity of gene variants observed in
263 patients with FTD or ALS will help to prioritise these variants for more intensive research
264 efforts into how they cause disease.

265

266 **Methods**

267 *DNA constructs*

268 *CYLD*, *TARDBP* and *FUS* mutations were introduced into the pCMV6-*CYLD*, pCMV6-
269 *TARDBP* and pCMV6-*FUS* constructs (Origene) by site-directed mutagenesis using the
270 QuikChange Lightning Site-Directed Mutagenesis Kit (Agilent). Mutated *CYLD* and
271 *TARDBP* cDNA sequences were then subcloned, using AsiSI and MluI restriction sites, into
272 the pCMV6-AC-GFP vector (Origene) for expression of C-terminal GFP-tagged *CYLD* and
273 TDP-43 proteins, respectively. Mutated *FUS* cDNA sequences were subcloned similarly into
274 the pCMV6-AN-GFP vector (Origene) for expression of N-terminal GFP-tagged *FUS*
275 protein, to avoid interference of the GFP tag with the C-terminal nuclear localisation signal of
276 the *FUS* protein [44]. All clones were verified by restriction digestion and sequence analysis.

277

278 *Cell Culture*

279 HEK293 and SH-SY5Y cell lines were used in this study. HEK293 cells were maintained in
280 Eagle's Minimum Essential Medium (EMEM; Gibco) and SH-SY5Y cells in Dulbecco's
281 Modified Eagle's Medium/Nutrient Mixture F-12 (DMEM/F12; 1:1 mixture; Gibco) each
282 containing 10% heat-inactivated fetal calf serum (Sigma-Aldrich). For
283 immunocytochemistry, 8-well chamber slides (Ibidi) were coated with (concentration) poly-

Oyston *et al* 2021

284 L-lysine (Sigma-Aldrich) for 1 h and then washed twice with Dulbecco's phosphate-buffered
285 saline (DPBS; Gibco). SH-SY5Y cells were seeded at 5– 7.5 x 10⁴ cells/well and HEK293
286 cells were seeded at 8 x 10⁴ cells/well. After 24 h, cells were transfected with GFP constructs
287 (250 ng/well) for 24 (HEK293) or 48 (SH-SY5Y) hours using Lipofectamine 3000 (0.75
288 L/well; Invitrogen) as per the manufacturer's protocol. For the staurosporine experiment,
289 cells were incubated for 48 h after seeding, then treated for 5 h with 0.1, 1 or 10 M
290 staurosporine (Sigma-Aldrich), to induce apoptosis. 100X staurosporine solutions were
291 prepared from a 1 mM staurosporine stock solution in dimethyl sulfoxide (DMSO), thus
292 DMSO was adjusted to a final concentration of 1% for control and lower staurosporine
293 concentrations.

294

295 *Immunocytochemistry*

296 Transfected and/or drug-treated cells were fixed in 4% paraformaldehyde (PFA) in PBS for
297 20 minutes in the dark. For visualisation of exogenous TDP-43 and FUS, cells were then
298 washed twice with DPBS and mounted using DAKO fluorescent mounting medium
299 containing 4',6-diamidino-2-phenylindole (DAPI; Agilent). For visualisation of endogenous
300 TDP-43 and FUS, non-specific background staining was blocked after cell fixation using 1%
301 bovine serum albumin (BSA) in PBS for 30 minutes. Cells were then incubated overnight at
302 4°C with rabbit anti-TDP-43 (1:500; Proteintech #10782-2-AP) or rabbit anti-FUS (1:500,
303 Proteintech #11570-1-AP) antibodies. The next day, cells underwent 2 x 5-minute washes
304 with DPBS, incubation with rabbit Alexa Fluor-647 secondary antibody (1:500; #A-21244)
305 for 1 hour, followed by 2 x 5-minute washes and mounting as above. Cells were imaged for
306 fluorescence intensity quantification with a 40x objective on a Nikon A1R confocal
307 microscope. Images of representative cells were obtained with a 100x objective for figure

Oyston *et al* 2021

308 preparation. Laser intensity, gain and offset settings were kept constant and at least five
309 random fields of view were imaged for each experiment.

310

311 *Fluorescence Intensity Quantification*

312 Quantification of changes in the cellular localisation of TDP-43 or FUS between the nucleus
313 and the cytoplasm was done by utilising CellProfiler 3.1.9 software (Broad Institute,
314 Cambridge, MA) [25]. To prepare images for analysis, ND2 microscope files were converted
315 to TIFFs, blinded and split into individual wavelength channel images using ImageJ
316 (National Institutes of Health, Bethesda MD). In CellProfiler, the DAPI channel was analysed
317 first using the *Identify Primary Objects* module and a global, three-class Otsu thresholding
318 method. This allowed for identification and separation of each nuclei within an image. Strict
319 filtering for cell diameter (30-60 pixels) eliminated any irregular or overlapped nuclei that
320 were present. TDP- or FUS-positive cells were also identified using the *Identify Primary*
321 *Objects* module. Cell diameter filtering for this step had a much larger range and was
322 dependent on experimental conditions and cell type (20-150 pixels). The *Relate* and *Filter*
323 modules were used to link filtered nuclei to TDP- or FUS-positive cells. Centroid distance
324 filtering, which limits the distance between the centre of the nucleus and the centre of the
325 cytoplasm (maximum 40 pixels) was also applied to remove any debris or abnormal cells that
326 may be fluorescing in the TDP-43/FUS channel. For the experiments quantifying endogenous
327 TDP-43 in cells expressing GFP-tagged CYLD constructs, additional steps in the analysis
328 were required. GFP-positive CYLD cells were identified in the same way as TDP- or FUS-
329 positive cells using the *Identify Primary Objects* module, described above. However, prior to
330 this, TDP-positive cells were identified by association with their corresponding nuclei, using
331 the *Identify Secondary Objects* module. The watershed-image method was used with global,

332 *Oyston et al 2021*

332 three-class Otsu thresholding. Size filtering was also applied (maximum 3000 pixels) to
333 remove any clumped cells. The *Relate* and *Filter* modules were used to select only TDP-
334 positive cells that were also positive for GFP. TDP- and GFP-positive cells were then linked
335 to their corresponding nuclei using the *Relate* and *Filter* modules described above. For all
336 experiments, in each TDP-43/FUS-positive cell, the nucleus and cytoplasm were separated
337 into individual objects using the *Identify Tertiary Objects* module. Integrated (total)
338 fluorescence intensity for both cellular compartments were then measured from the TDP-
339 43/FUS channel image using the *Measure Object Intensity* module. Using these
340 measurements, the cytoplasmic to nuclear ratio of TDP-43 or FUS was calculated for 300
341 cells per group, for each of the six replicates of the experiment. All filtering and thresholding
342 steps in each experimental pipeline were kept consistent throughout all experimental
343 replicates. Filtering values were specific to each experiment and require adjustment for
344 different cell types and microscope parameters.

345

346 *Statistical Analysis*

347 Data are presented as mean \pm standard error of the mean (SEM) from at least six independent
348 experiments. Mean fluorescent intensity of TDP-43 or FUS across six biological replicates
349 was in most cases compared by repeated measures one-way ANOVA and Dunnett's multiple
350 comparisons test. The effect of CYLD on endogenous TDP-43 was analysed using repeated
351 measures one-way ANOVA and Sidak's multiple comparisons test. All statistical analyses
352 were performed using GraphPad Prism 9. Significance for all tests was set at $p < 0.05$.

353

354 **Abbreviations**

355 *Oyston et al 2021*

355 ALS: amyotrophic lateral sclerosis; BSA: bovine serum albumin; DAPI: 4',6-diamidino-2-
356 phenylindole; DMEM: Dulbecco's modified Eagle's medium; DMSO: dimethyl sulfoxide;
357 DPBS: Dulbecco's phosphate-buffered saline; EMEM: Eagle's minimum essential medium;
358 FTD: frontotemporal dementia; FUS: fused in sarcoma; F12: nutrient mixture F-12; GFP:
359 green fluorescent protein; HEK293: human embryonic kidney; PFA: paraformaldehyde;
360 SEM: standard error of the mean; TDP-43: TAR DNA-binding protein 43; WT: wild-type.

361 **Declarations**

362 *Ethics approval and consent to participate*

363 Not applicable.

364

365 *Consent for publication*

366 Not applicable.

367

368 *Availability of data and materials*

369 The datasets and materials generated during the current study are available from the
370 corresponding author on reasonable request.

371

372 *Competing interests*

373 The authors declare that they have no competing interests.

374

375 *Funding*

376 This research was funded by the National Health & Medical Research Council of Australia
377 (NHMRC) Project Grant 1140708 (to CDS & JBK), by NHMRC Boosting Dementia
378 Research Leadership Fellowship 1138223 (to CDS) and the University of Sydney. JBK is
379 supported by NHMRC Project Grant 1163249, NHMRC-JPND Grant 1151854 and NHMRC

Oyston *et al* 2021

380 Dementia Research Team Grant 1095127.

381

382 *Authors' contributions*

383 LJO, JBK and CDS conceived the study. SU, LF, MH and LMB generated and sequence-
384 verified mutant cDNA constructs. LJO carried out TDP-43 and FUS localisation experiments.
385 LJO and CDS participated in data analysis. LJO and CDS drafted the manuscript. All authors
386 read and approved the final manuscript.

387

388 *Acknowledgements*

389 The authors acknowledge the facilities and technical assistance of Microscopy Australia at
390 the Australian Centre for Microscopy & Microanalysis at the University of Sydney.

391

392 **References**

- 393 1. Lillo P, Hodges JR (2009) Frontotemporal dementia and motor neurone disease:
394 Overlapping clinic-pathological disorders. *J Clin Neurosci* 16:1131–1135
- 395 2. Burrell JR, Halliday GM, Kril JJ, Ittner LM, Götz J, Kiernan MC, Hodges JR (2016)
396 The frontotemporal dementia-motor neuron disease continuum. *Lancet* 388:919–931
- 397 3. Abramzon YA, Fratta P, Traynor BJ, Chia R (2020) The Overlapping Genetics of
398 Amyotrophic Lateral Sclerosis and Frontotemporal Dementia. *Front Neurosci* 14:1–10
- 399 4. Dobson-Stone C, Hallupp M, Shahheydari H, et al (2020) CYLD is a causative gene
400 for frontotemporal dementia - amyotrophic lateral sclerosis. *Brain* 143:783–799
- 401 5. Prasad A, Bharathi V, Sivalingam V, Girdhar A, Patel BK (2019) Molecular
402 mechanisms of TDP-43 misfolding and pathology in amyotrophic lateral sclerosis.
403 *Front Mol Neurosci* 12:1–36

Oyston *et al* 2021

404 6. Mackenzie IRA, Rademakers R, Neumann M (2010) TDP-43 and FUS in amyotrophic
405 lateral sclerosis and frontotemporal dementia. *Lancet Neurol* 9:995–1007

406 7. Vance C, Rogelj B, Hortobágyi T, et al (2009) Mutations in FUS, an RNA processing
407 protein, cause familial amyotrophic lateral sclerosis type 6. *Science* (80-) 323:1208–
408 1211

409 8. Mackenzie IRA, Munoz DG, Kusaka H, Yokota O, Ishihara K, Roeber S, Kretzschmar
410 HA, Cairns NJ, Neumann M (2011) Distinct pathological subtypes of FTLD-FUS.
411 *Acta Neuropathol* 121:207–218

412 9. Neumann M, Sampathu DM, Kwong LK, et al (2006) Ubiquitinated TDP-43 in
413 Frontotemporal Lobar Degeneration and Amyotrophic Lateral Sclerosis. *Science* (80-)
414 314:130–133

415 10. Cairns NJ, Bigio EH, Mackenzie IRA, et al (2007) Neuropathologic diagnostic and
416 nosologic criteria for frontotemporal lobar degeneration: Consensus of the Consortium
417 for Frontotemporal Lobar Degeneration. *Acta Neuropathol* 114:5–22

418 11. Sreedharan J, Blair IP, Tripathi VB, et al (2008) TDP-43 Mutations in Familial and
419 Sporadic Amyotrophic Lateral Sclerosis. *Science* (80-) 319:1668–1672

420 12. Kwiatkowski TJ, Bosco DA, LeClerc AL, et al (2009) Mutations in the FUS/TLS gene
421 on chromosome 16 cause familial amyotrophic lateral sclerosis. *Science* (80-)
422 323:1205–1208

423 13. Lagier-tourenne C, Polymenidou M, Cleveland DW (2010) TDP-43 and FUS / TLS□:
424 emerging roles in RNA processing and neurodegeneration. 19:46–64

425 14. Brown RH, Al-Chalabi A (2017) Amyotrophic Lateral Sclerosis. *N Engl J Med*
426 377:162–172

427 15. Younes K, Miller BL (2020) Frontotemporal Dementia: Neuropathology, Genetics,
428 Neuroimaging, and Treatments. *Psychiatr Clin North Am* 43:331–344

Oyston *et al* 2021

429 16. Deng Q, Holler CJ, Taylor G, et al (2014) FUS is phosphorylated by DNA-PK and
430 accumulates in the cytoplasm after DNA damage. *J Neurosci* 34:7802–7813

431 17. Naumann M, Pal A, Goswami A, et al (2018) Impaired DNA damage response
432 signaling by FUS-NLS mutations leads to neurodegeneration and FUS aggregate
433 formation. *Nat Commun.* <https://doi.org/10.1038/s41467-017-02299-1>

434 18. Walker AK, Soo KY, Sundaramoorthy V, et al (2013) ALS-associated TDP-43
435 induces endoplasmic reticulum stress, which drives cytoplasmic TDP-43 accumulation
436 and stress granule formation. *PLoS One* 8:1–12

437 19. Han JH, Yu TH, Ryu HH, Jun MH, Ban BK, Jang DJ, Lee JA (2013) ALS/FTLD-
438 linked TDP-43 regulates neurite morphology and cell survival in differentiated
439 neurons. *Exp Cell Res* 319:1998–2005

440 20. Kabashi E, Lin L, Tradewell ML, et al (2009) Gain and loss of function of ALS-related
441 mutations of TARDBP (TDP-43) cause motor deficits in vivo. *Hum Mol Genet*
442 19:671–683

443 21. Wobst HJ, Wesolowski SS, Chadchankar J, Delsing L, Jacobsen S, Mukherjee J, Deeb
444 TZ, Dunlop J, Brandon NJ, Moss SJ (2017) Cytoplasmic Relocalization of TAR DNA-
445 Binding Protein 43 Is Not Sufficient to Reproduce Cellular Pathologies Associated
446 with ALS In vitro. *Front Mol Neurosci* 10:1–13

447 22. Arnold ES, Ling S-C, Huelga SC, et al (2013) ALS-linked TDP-43 mutations produce
448 aberrant RNA splicing and adult-onset motor neuron disease without aggregation or
449 loss of nuclear TDP-43. *Proc Natl Acad Sci* 110:E736–E745

450 23. Araki W, Minegishi S, Motoki K, Kume H, Hohjoh H, Araki YM, Tamaoka A (2014)
451 Disease-Associated Mutations of TDP-43 Promote Turnover of the Protein Through
452 the Proteasomal Pathway. *Mol Neurobiol* 50:1049–1058

453 24. Mutihac R, Alegre-Abarrategui J, Gordon D, Farrimond L, Yamasaki-Mann M, Talbot

Oyston *et al* 2021

454 K, Wade-Martins R (2015) TARDBP pathogenic mutations increase cytoplasmic
455 translocation of TDP-43 and cause reduction of endoplasmic reticulum Ca²⁺ signaling
456 in motor neurons. *Neurobiol Dis* 75:64–77

457 25. Carpenter AE, Jones TR, Lamprecht MR, et al (2006) CellProfiler: Image analysis
458 software for identifying and quantifying cell phenotypes. *Genome Biol.*
459 <https://doi.org/10.1186/gb-2006-7-10-r100>

460 26. Bosco DA, Lemay N, Ko HK, Zhou H, Burke C, Kwiatkowski TJ, Sapp P, Mckenna-
461 Yasek D, Brown RH, Hayward LJ (2010) Mutant FUS proteins that cause amyotrophic
462 lateral sclerosis incorporate into stress granules. *Hum Mol Genet* 19:4160–4175

463 27. Gitcho MA, Baloh RH, Chakraverty S, et al (2008) TDP-43 A315T mutation in
464 familial motor neuron disease. *Ann Neurol* 63:535–538

465 28. Buratti E (2015) Functional Significance of TDP-43 Mutations in Disease. *Adv Genet*
466 91:1–53

467 29. Kabashi E, Valdmanis PN, Dion P, et al (2008) TARDBP mutations in individuals
468 with sporadic and familial amyotrophic lateral sclerosis. *Nat Genet* 40:572–574

469 30. Rutherford NJ, Zhang YJ, Baker M, et al (2008) Novel mutations in TARDBP(TDP-
470 43) in patients with familial amyotrophic lateral sclerosis. *PLoS Genet* 4:1–8

471 31. Bignell GR, Warren W, Seal S, et al (2000) Identification of the familial
472 cylindromatosis tumour-suppressor gene. *Nat Genet* 25:160–165

473 32. Rajan N, Ashworth A (2015) Inherited cylindromas: Lessons from a rare tumour.
474 *Lancet Oncol* 16:e460–e469

475 33. Kim SH, Zhan L, Hanson KA, Tibbetts RS (2012) High-content RNAi screening
476 identifies the type 1 inositol triphosphate receptor as a modifier of TDP-43 localization
477 and neurotoxicity. *Hum Mol Genet* 21:4845–4856

478 34. Kim M, Kim HJ, Koh W, et al (2020) Modeling of frontotemporal dementia using

Oyston *et al* 2021

479 IPSC technology. *Int J Mol Sci* 21:1–16

480 35. Van Langenhove T, van der Zee J, Sleegers K, et al (2010) Genetic contribution of
481 FUS to frontotemporal lobar degeneration. *Neurology* 74:366–71

482 36. Broustal O, Camuzat A, Guillot-Noël L, et al (2010) FUS mutations in frontotemporal
483 lobar degeneration with amyotrophic lateral sclerosis. *J Alzheimers Dis* 22:765–769

484 37. Acosta JR, Goldsbury C, Winnick C, et al (2014) Mutant human FUS is ubiquitously
485 mislocalized and generates persistent stress granules in primary cultured transgenic
486 zebrafish cells. *PLoS One*. <https://doi.org/10.1371/journal.pone.0090572>

487 38. Moreno F, Rabinovici GD, Karydas A, et al (2015) A novel mutation P112H in the
488 TARDBP gene associated with frontotemporal lobar degeneration without motor
489 neuron disease and abundant neuritic amyloid plaques. 1–13

490 39. Van Deerlin VM, Leverenz JB, Bekris LM, et al (2008) TARDBP mutations in
491 amyotrophic lateral sclerosis with TDP-43 neuropathology: a genetic and
492 histopathological analysis. *Lancet Neurol* 7:409–416

493 40. Gelpi E, van der Zee J, Turon Estrada A, Van Broeckhoven C, Sanchez-Valle R (2014)
494 TARDBP mutation p.Ile383Val associated with semantic dementia and complex
495 proteinopathy. *Neuropathol Appl Neurobiol* 40:225–230

496 41. Gitcho MA, Bigio EH, Mishra M, et al (2009) TARDBP 3'-UTR variant in autopsy-
497 confirmed frontotemporal lobar degeneration with TDP-43 proteinopathy. *Acta
498 Neuropathol* 118:633–645

499 42. Pansarasa O, Bordoni M, Drufuca L, et al (2018) Lymphoblastoid cell lines as a model
500 to understand amyotrophic lateral sclerosis disease mechanisms. *DMM Dis Model
501 Mech* 11:1–12

502 43. Gianini M, Bayona-Feliu A, Sproviero D, Barroso SI, Cereda C, Aguilera A (2020)
503 TDP-43 mutations link Amyotrophic Lateral Sclerosis with R-loop homeostasis and R

Oyston et al 2021

504 loopmediated DNA damage. PLoS Genet 16:1–23

505 44. Vance C, Scotter EL, Nishimura AL, et al (2013) ALS mutant FUS disrupts nuclear

506 localization and sequesters wild-type FUS within cytoplasmic stress granules. Hum

507 Mol Genet 22:2676–2688

508

Oyston *et al* 2021

509

510 **Figure Legends**

511 **Fig. 1 Detection of FUS cytoplasmic mislocalisation with exogenous expression of FUS**

512 **mutations.** Representative images of SH-SY5Y cells overexpressing GFP-tagged **(a-c)**

513 **FUS_{WT}, (e-g) FUS_{R521C} or (i-k) FUS_{R495X}.** Nuclei were visualised with DAPI (blue). **(d)**

514 Quantification of the fluorescence intensity of the nucleus shows a significant reduction in

515 nuclear FUS expression in cells expressing FUS_{R521C} or FUS_{R495X}, when compared to FUS_{WT}.

516 **(h)** Quantification of the fluorescence intensity of cytoplasmic FUS shows significantly higher

517 cytoplasmic FUS expression in FUS_{R521C} and FUS_{R495X}, when compared to FUS_{WT}. **(l)**

518 Quantification of the cytoplasmic/nuclear ratio of exogenous FUS shows a marked increase

519 in FUS_{R521C}- and FUS_{R495X}-expressing cells when compared to FUS_{WT}. Scale bars = 5 μm.

520 Data is represented as mean ± SEM. a.u. = arbitrary units. *p<0.05; **p<0.01; ***p<0.001;

521 ****p<0.0001.

522

523 **Fig. 2 Detection of endogenous FUS cytoplasmic mislocalisation following staurosporine**

524 **treatment. (a-d)** Representative fluorescence images of SH-SY5Y cells treated with

525 increasing concentrations of staurosporine. FUS was detected by immunofluorescent

526 staining (red) and nuclei were visualised with DAPI (blue). **(e)** Quantification of nuclear and

527 **(f)** cytoplasmic FUS fluorescence intensity show significant changes in 1 μM- and 10 μM-

528 treated cells. **(g)** Quantification of the FUS cytoplasmic/nuclear ratio shows an increase in all

529 treatment groups when compared to those treated with DMSO alone. Scale bars = 20 μm.

530 Data is represented as mean ± SEM. a.u. = arbitrary units. *p<0.05; **p<0.01; ***p<0.001.

531

532 **Fig. 3 Detection of TDP-43 cytoplasmic mislocalisation with exogenous expression of**

533 **TARDBP mutations.** Representative images of SH-SY5Y cells overexpressing GFP-tagged

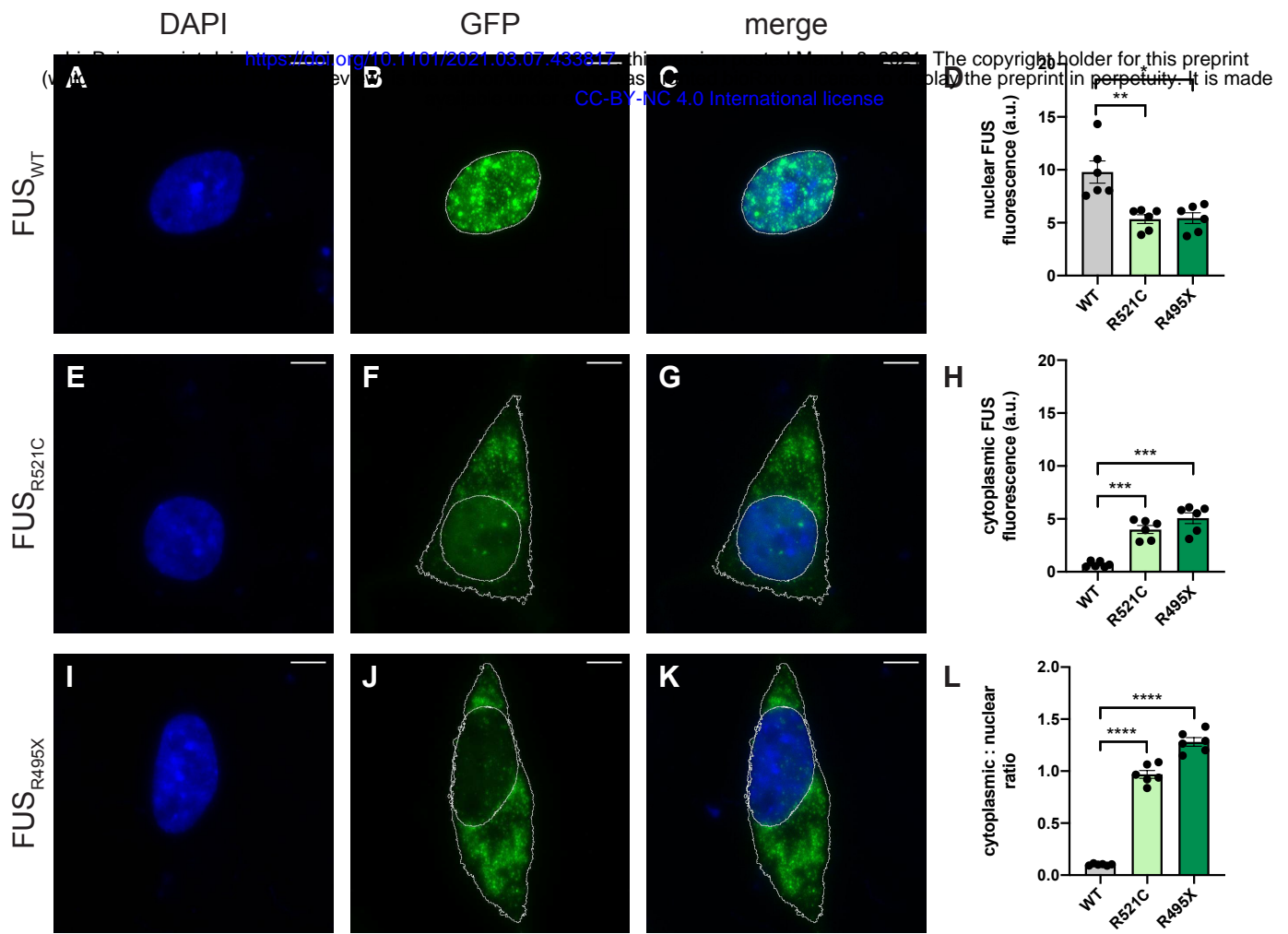
534 *Oyston et al 2021*

534 **(a, e)** TDP-43_{WT}, **(b, f)** TDP-43_{A315T}, **(c, g)** TDP-43_{M337V} or **(d, h)** TDP-43_{A382T}. Nuclei were
535 visualised with DAPI (blue). **(i)** Quantification of the fluorescence intensity of the nucleus
536 and **(j)** the cytoplasm shows no significant difference in TDP-43 expression. **(k)**
537 Quantification of the cytoplasmic/nuclear ratio of exogenous TDP-43 shows a significant
538 increase in TDP-43_{A315T} and TDP-43_{A382T}, and a decrease in TDP-43_{M337V}, when compared to
539 cells expressing TDP-43_{WT}. Scale bars = 5 μm. Data is represented as mean ± SEM. a.u. =
540 arbitrary units. **p<0.01.

541

542 **Fig. 4 Detection of endogenous TDP-43 cytoplasmic mislocalisation in cells expressing**
543 **CYLD mutations.** Representative images of SH-SY5Y cells overexpressing **(a-d)** GFP or
544 GFP-tagged **(e-h)** CYLD_{WT}, **(i-l)** CYLD_{D681G} or **(m-p)** CYLD_{M719V}. TDP-43 was detected by
545 immunofluorescent staining (red) and nuclei were visualised with DAPI (blue). **(q)**
546 Quantification of the fluorescence intensity of the nucleus shows no difference in TDP-43
547 expression. **(r)** Quantification of cytoplasmic TDP-43 fluorescence intensity shows increased
548 TDP-43 expression in CYLD_{WT}, when compared to GFP and CYLD_{M719V}, when compared to
549 CYLD_{WT}. **(s)** Quantification of the cytoplasmic/nuclear ratio of exogenous TDP-43 shows a
550 marked increase in CYLD_{WT}, when compared to cells expressing GFP. The
551 cytoplasmic/nuclear ratio of TDP-43 in CYLD_{M719V}-expressing cells was significantly higher
552 than CYLD_{WT}. Scale bars = 5 μm. Data is represented as mean ± SEM. a.u. = arbitrary units.
553 ***p<0.001; ****p<0.0001.

554



Staurosporine Concentration (μM)

bioRxiv preprint doi: <https://doi.org/10.1101/2021.03.07.433817>; this version posted March 8, 2021. The copyright holder for this preprint (which was not certified by peer review) is the author/funder, who has granted bioRxiv a license to display the preprint in perpetuity. It is made available under aCC-BY-NC 4.0 International license.

